Y PHOTOCATALYSTS IN CERAMICS

S. Cerro, R. Galindo, A. García, A. Monrós, J. Badenes, C. Gargori, G. Monrós.

Unit for Environmental Inorganic Chemistry and Ceramic Materials, Dept. of Inorganic and Organic Chemistry, Universidad Jaume I, Castellón (Spain).

ABSTRACT

Advanced oxidation processes (AOPs) are oxidation processes based on sufficient concentrations of hydroxyl radicals to degrade dissolved organic compounds present in water or those that are dispersed in air to mineral forms or at least to harmless organic compounds. It is a safe and clean technology and, in certain processes, solar radiation can be used as process initiator. Titanium oxide is currently the reference as photocatalytic material, given its high activity, relative stability, low cost, and low toxicity. In this study, the use of 'ceramic' photocatalysts (ceramic composites) in treatment processes for specific pollutants in urban environments (VOCs and NOx) and wastewaters (persistent, bioaccumulative and toxic (PBT) organic compounds) is analysed, as well as their use 'in ceramics' on glazed ceramic tiles as substrates for photocatalytic layers or photocatalytic glazes.

1. INTRODUCTION

So-called advanced oxidation processes (AOPs) are oxidation processes based on sufficient concentrations of hydroxyl radicals to degrade the dissolved organic compounds present in water or those that are dispersed in air to mineral forms or at least to harmless organic compounds. The OH· radical is the most important natural oxidant in tropospheric chemistry (1). It is often termed the 'detergent' of the atmosphere, as it reacts with many pollutants, initiating their cleaning process, while it also plays an important role in the elimination of greenhouse gases such as methane or ozone. The features that make AOPs attractive are, among others, that they break up the pollutant, which is not concentrated or transferred to another medium, providing complete or almost complete mineralisation of the organic pollutants, and can serve in breaking up the immense majority of organic compounds, especially non-biodegradable compounds such as organochlorated compounds, PCBs, PAHs, etc. It is a safe and clean technology and, in certain processes, solar radiation can be used as process initiator.

Titanium oxide is currently the photocatalyst material of reference, given its high activity, relative stability, low cost, and low toxicity. However, certain problems need to be addressed such as the low velocity of photocatalysis, generation of toxic degradation intermediates, deactivation of the material, and need for UV irradiation as its band gap does not match that of sunlight: the use of ceramic composites could enhance these aspects (2).

Fukaya studied the removal of NOx from ambient air using ceramic blocks impregnated with a TiO_2 film. This provided removal of 94 and 98% NO_x, using various blocks with single and triple impregnation, respectively. Ichiura (3) also studied the photocatalytic oxidation of NO_x on titanium dioxide sheets modified with metallic composites.

2. OBJECTIVES

This paper presents examples of the use of 'ceramic' photocatalysts (ceramic composites) in the treatment processes of specific pollutants in urban environments (VOCs and NOx) and wastewaters (PBT organic compounds), as well as the use 'in ceramics' of glazed ceramic tiles as substrates for photocatalytic layers or photocatalytic glazes (4).

3. CERAMIC COMPOSITES APPLIED TO THE TREATMENT OF NOX AND VOCS

Studies on the presence of VOCs in residential, transport, or office environments indicate that cleaning agents introduce high rates of acetone and ethanol, perfumes limonene, and rests of dry-cleaning products tetrachloroethylene and

xylenes. These compounds display hazardous properties, such as toxicity and carcinogenicity, and are also tropospheric ozone precursors (Table I).

Compound	Plane cockpit	Residential	Office
Acetone	41-60	**32-130**	--
Benzene	0-6	8-34	5-12
Ethanol	**324-1116**	120-490	--
Formaldehyde	5-9	--	**11-66**
Limonene	30-62	**21-450**	6
Dichloromethane	**122**	--	3-10
Tetrachloroethylene	4-5	**7-65**	3-14
Toluene	7-68	**37-320**	6-58
m/p-xylene	3-5	**18-120**	5-37

Table I. *Presence of volatile organic compounds (VOCs) (μg/Nm³) in internal environments (5).*

Inorganic pollutants such as nitrogen oxides NO_x also appear in the air, which are precursors, together with VOCs, of oxidising agents such as peroxyacyl nitrates (PAN) and of tropospheric ozone, as well as triggering acid rain in the presence of SO_2. These compounds are generated fundamentally by reaction between nitrogen and oxygen in the air, on being subjected to high temperatures such as those of car combustion engines. Wastewater degradation processes produce hydrosulphuric acid or hydrogen sulphide H_2S, with a sickening smell of rotten eggs, which is already noticeable at concentrations above 5 ppb. In the European Union, the presence of NO_x is limited to a maximum of 200 μg/Nm³ in one hour and 40 μg/Nm³ as annual average. In addition to these gaseous compounds there are also others of an inorganic nature associated with suspended particles, whose PM10 (size below 10 μm) fraction is limited to a daily average of 50 (which may only be exceeded 35 days a year), while the PM2.5 (size below 2.5 μm) fraction is limited to an annual average of 40, these being particles that can easily reach and enter the lung alveoli. The so-called nanoparticles or UFPs (ultrafine particles) with a size below 0.1 μm (100 nm) are also being studied, for their control and limitation, since their nanometric size enables them to pass directly into the bloodstream from the lung alveoli. Many of these particles are made up of heavy metals such as Cu and Sb (stemming from the wear of car brake shoes; in the air in Madrid up to 90 ng/Nm³ of Cu may be measured, whereas in Huelva, where copper is mined and processed, only 70 ng/Nm³ of Cu is measured), or Zn (from tyre wear). These particles can also bear important adsorbed concentrations of VOCs (6).

It should be noted that chemistry in the atmosphere, just as all 'natural chemistry' is directed more by photolysis (interaction of photons) than by thermal excitation: in effect, the binding energies of oxygen and chlorine, or C-H, O-H, and

C-O bonds are of the order of 495 kJ/mol (O_2), 243 kJ/mol (Cl_2), and ~ 400 kJ/mol, respectively, which are difficult to reach by thermal collision (E=RT=8.3T J/mol, of the order of only 2.5kJ/mol at 300K) but which may be achieved by interaction of photons of the visible spectrum (E=hv of 190 kJ/mol for a yellow photon of 600 nm) and even more so with ultraviolet photons (380 kJ/mol for 300 nm).

Figure 1. Irradiation with a mercury UV lamp of 60 W maintaining an air flow of 6 l/min through the photocatalyst for 48 hours.

Photocatalytic oxidation of NO_x by anatase has been widely studied (7). With a view to monitoring the photocatalysis of nitrogen oxide collection from the air by nitrate oxidation, 2.00 g (M1) of dry test photocatalyst was charged in a funnel closed with cotton wool and irradiated with a mercury UV lamp of 60 W maintaining an air flow of 6 l/min through the photocatalyst for 48 hours (Figure 1). The funnel was dried in an oven at 110ºC for 12 h and weighed (M2), measuring the possible mass variation M2-M1. The irradiated photocatalyst was washed by running 10 ml water through the funnel, and the nitrate content in the washing water was measured by colorimetry at 250 nm. Once the average NO_x concentration in the treated air had been determined, the collection efficiency E(%) could be estimated.

Ceramic composites of composition SiO_2-TiO_2 were prepared by sol-gel methods from precursors alkoxide TEOS (Si) and titanium isopropoxide (Ti), all supplied by ALDRICH and analysis grade. Figure 2.a shows a binocular magnifying glass micrograph (x40) of the dry gel and the UV-Vis-NIR spectrum of the composite. Figure 3 presents its X-ray diffraction.

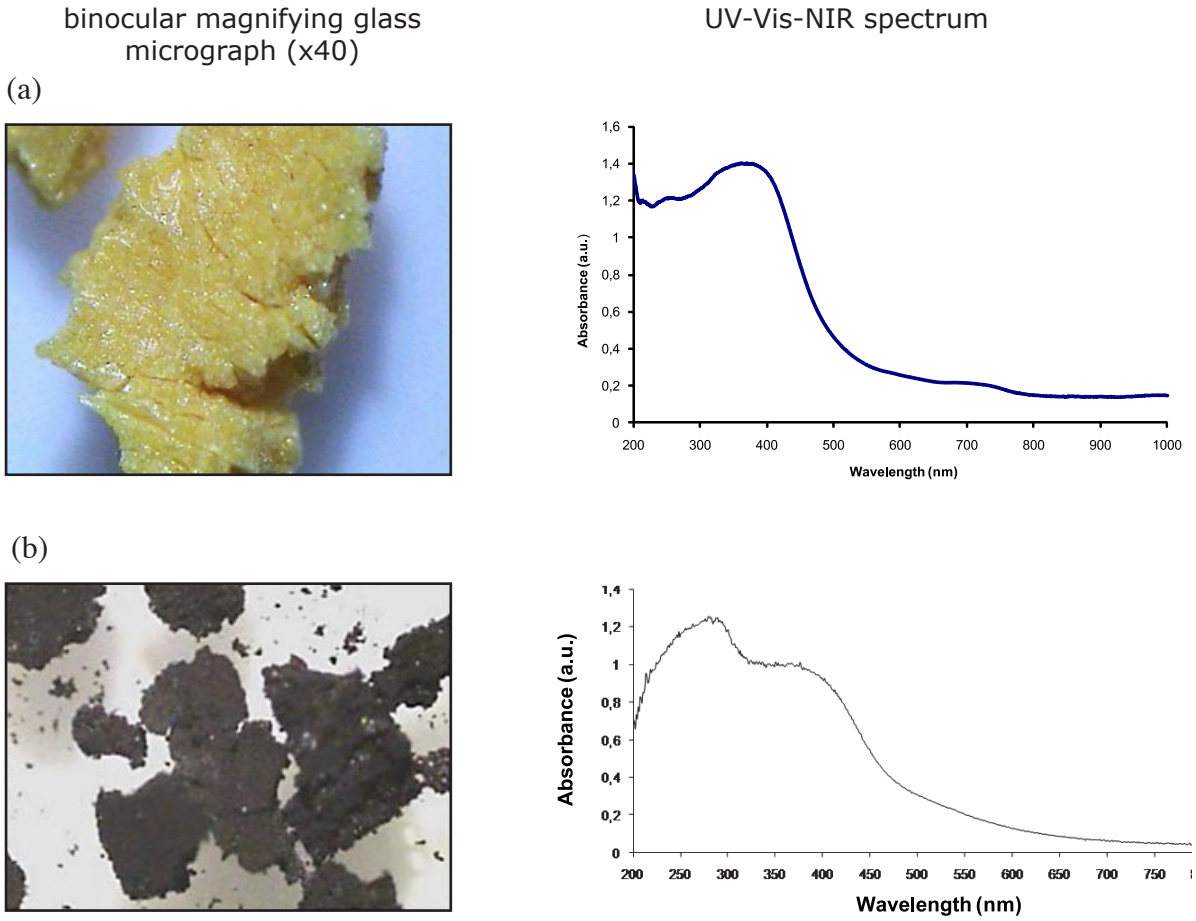

Figure 2. Binocular magnifying glass micrograph (x40) of the dry gel, its X-ray diffraction, and the UV-Vis-NIR spectrum of: (a) SiO_2-TiO_2 composite, (b) Si-Mn composite.

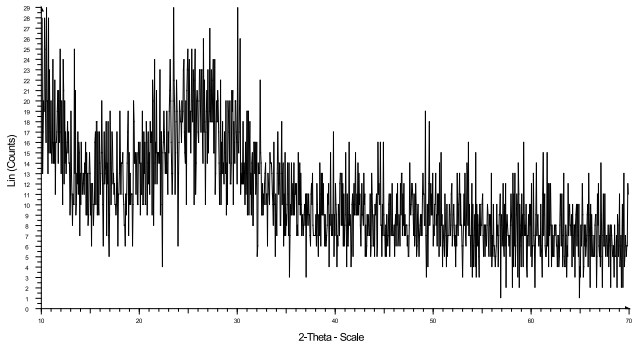

Figure 3. X-ray diffraction and UV-Vis-NIR spectrum of the SiO_2-TiO_2 composite.

The glassy appearance and intense yellow colour of the resulting gels can be observed in Figure 2, while the UV-Vis-NIR spectrum indicates the presence of two charge transfer bands in composite SiO_2-TiO_2 centred at 270 and 380 nm respectively, which provide the material with a semiconducting character and band gap of 2.48 eV. A strong amorphous halo centred at 25º2θ may be observed in the X-ray diffractogram of Figure 3, which is usual in these materials.

The photocatalytic capability of the composites on the photo-oxidation of nitrogen oxides was studied according to the methodology described previously. Table II presents the results of the photo-oxidation test.

SAMPLE	ΔM(g)	$[NO_3^-]$ (ppm)	E(%)
SiO_2-TiO_2	-0.02	4.9	7
SiO_2-MnO_2	-0.01	44.2	63

Table II. Photocatalytic capability of composites on the photo-oxidation of nitrogen oxides.

The results in Table II indicate a discreet efficiency in the oxidation of NO_x oxides of the order of 7%. However, in a silica gel sensibilised with 0.1 mol manganese by weight formula (Si-Mn), this displays an estimated collection efficiency of 63%. Once they had dried, the Si-Mn gels stabilised at 300ºC for 1 hour, displaying the dark brown appearance shown in Figure 2.a in the binocular magnifying glass, with a Si^{4+}-O^{2-} charge transfer band, centred at 290 nm and another band associated with the manganese sensibiliser, already in the visible spectrum, at 370 nm (Fig. 2b). The band gap associated with the UV band absorption threshold is 3 eV and the band gap associated with the absorption of the sensibiliser in the visible spectrum is 2.4 eV.

4. CERAMIC COMPOSITES APPLIED TO THE TREATMENT OF PBT COMPOUNDS IN WASTEWATERS

PBTs or persistent, bioaccumulative and toxic chemicals are described in regulation (EC) no. 1907/2006 of the European parliament and of the Council of 18 December 2006 on the registration, evaluation, authorisation, and restriction of chemicals (REACH REGULATION). The objective of the REACH regulation is to achieve appropriate safety knowledge of substances sold in quantities of more than 1 ton, by REGISTRATION, through the performance of a thorough 'Chemical Safety Report' (REACH Annex I, and Annex X in which the analysis protocols are set out), by producers or importers of the substances in accordance with timelines that will end on 31 May 2018 with the registration of 'type 3 substances' of which more than 1 t/year is sold, and which are not PBTs (persistent, bioaccumulative, and toxic chemicals) o vPvB (very persistent and very bioacumulable), which in the current terminology include at least the category 1 or 2 CMRs of which more than 1 t/year is sold and the R50/53 (Very toxic to aquatic organisms, may cause long-term adverse effects in the aquatic environment) of which more than 100 t/year are sold.

The photocatalytic methods exhibit an interesting degradation efficiency for these persistent compounds. The persistent acid Orange II, a sulphonated mo-

noazo dye $C_{16}H_{11}N_2SO_4Na$ is used as model dye in photocatalytic photodegradation studies. The degradation mechanism of this compound is well described in the literature (8). To monitor the photodegradation kinetics of the substrates, the assembly shown in Figure 4.a was prepared, with a 125 W medium-pressure mercury lamp, with an emission spectrum that exhibited three characteristic lines at 254, 313, and 365 nm, used as UV radiation source on the solution contained in a quartz glass reactor (which minimises UV radiation filtering from the source) with a water-cooled sleeve. Solutions of the Orange II monoazo dye were used with a concentration of $0.6 \cdot 10^{-4}$ M buffered at pH 7.4 with a mixture of $NaH_2PO_4 \cdot 4H_2O$ and $Na_2HPO_4 \cdot 7H_2O$ (Panreac, S.A.) to which the powder photocatalyst was added in stirred suspensions of 500 mg/l. The Orange II degradation was monitored by colorimetry at 480 nm. The photodegradation curves were analysed according to the Langmuir-Hinshelwood model (4). In some cases methylene blue, which is less persistent and undergoes photolysis relatively easily, was used with the same concentration and irradiation pH.

A good photocatalyst with relation to Orange II could be the titanium oxide composite sensibilised with 0.1 mol manganese and 0.2 mol bipyridine with the precursors used previously and bipyridine. The glassy appearance and orange yellow colour of the resulting gels are shown in Figure 5. The UV-Vis-NIR spectrum displays the Ti^{4+}-O^{2-} charge band transfer at 290 nm and another band associated with manganese(II), already in the visible spectrum at 380 nm. The band gap associated with the absorption threshold of UV band is 3.8 eV and the band gap associated with the sensibilising absorption in the visible spectrum is 2.5 eV.

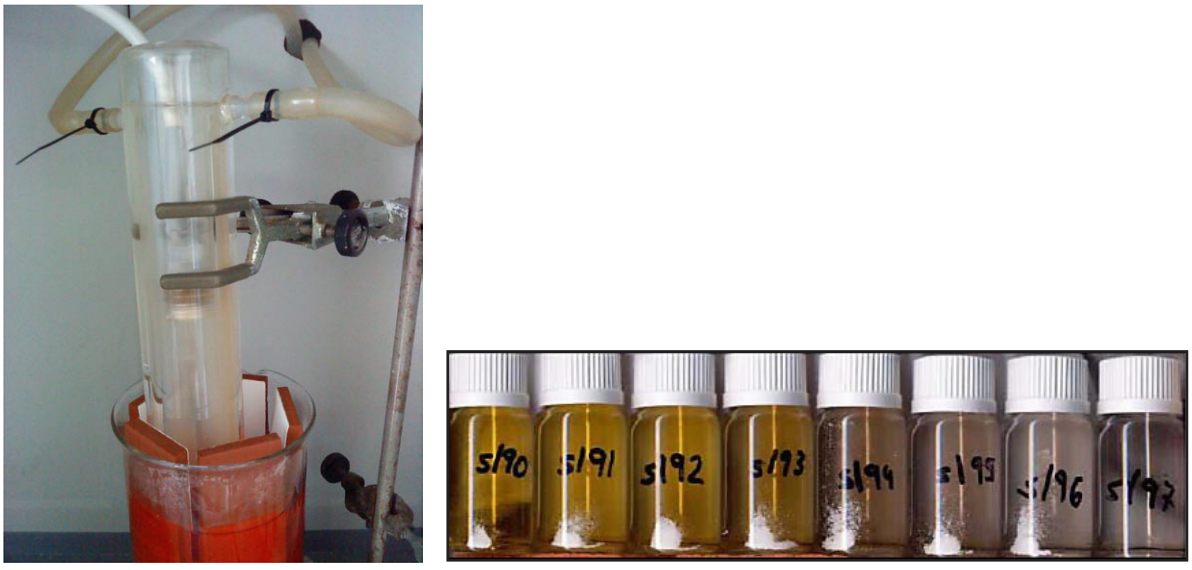

(a) (b)

Figure 4. Assembly prepared to determine the photodegradation kinetics and evolution of colour intensity of an Orange II solution as a function of time on its travel through the assembly

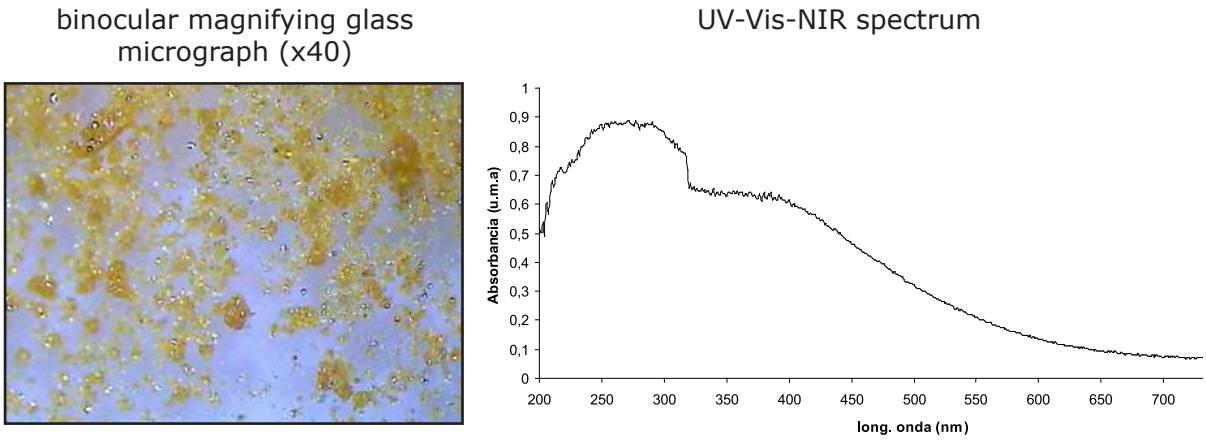

Figure 5. Binocular magnifying glass micrograph (x40) of the dry gel and UV-Vis-NIR spectrum of the Ti-Mn-Bipyridine composite.

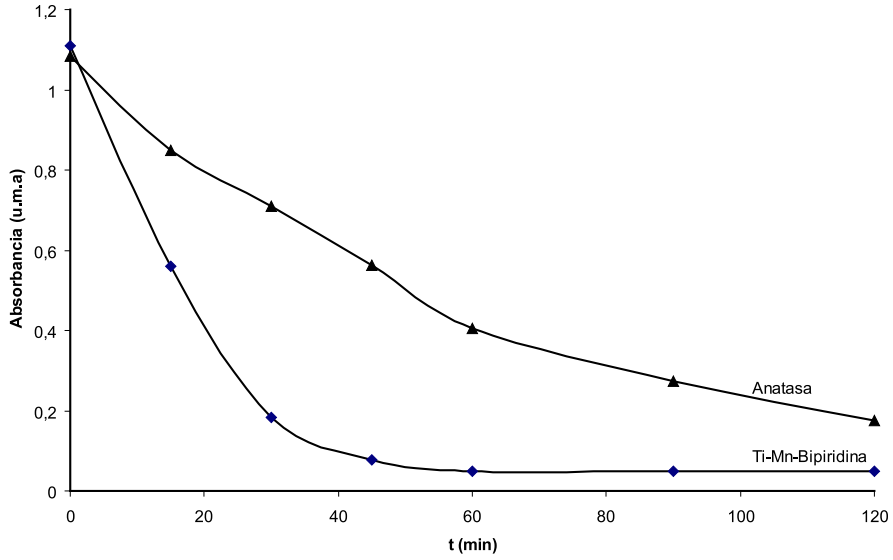

Figure 6. Orange II photodegradation curves of the Ti-Mn-Bipyridine composite and of the reference Anatase.

The Orange II photodegradation curves of the Ti-Mn-Bipyridine composite and of the reference Anatase are shown in Figure 6. The composite sensibilised with manganese-bipyridine exhibited a greater photodegradation capability than the anatase: the half-life time of Orange II was 17 min with the composite compared to 45 min with the reference anatase.

5. CERAMIC TILES WITH A PHOTOCATALYTIC SURFACE

The use of ceramic powders in the degradation processes of PBTs described above requires recovery of the photocatalyst in a batch operation. The use of a photocatalyst on a ceramic tile substrate allows the tedious photocatalyst recovery steps with the material losses always entailed by this operation to be suppressed, and the operation even to be performed continuously. The tests with ceramic tiles were conducted using the assembly described above, but with the tiles immersed, surrounding the solution to be irradiated as shown in Figure 4. It may be noted that when powders are used, whose specific surface area ranges from 5 to 100 m^2/g, in the worst of cases, the photocatalytic interaction surface in the photodegradation test is of the order of 0.3 m^2; in contrast, when tiles are immersed, the contact surface is only of the order of 0.03 m^2. Two options are available for photocatalysts on ceramic tile substrates: (a) as a photocatalytic film and (b) in the form of a conventional photocatalytic glaze coating. Some examples are described below.

5.1. Tile with deposition of a photocatalytic film

In a suitably stabilised polyethylene glycol medium, starting with soluble salts of tin, inks were prepared that, applied by screen printing with a screen mesh of 120 threads/cm^2, deposited cassiterite films with a tin percentage, measured as SnO_2, in the ink of 0.2, 0.6, 1, 2, 4, and 7%. Figure 7.e shows some of these coatings after firing, which displayed a glossy metallised appearance. The grazing-angle diffractograms of the samples with 4 and 7% cassiterite in the ink are shown in Figure 7.a; highly defined cassiterite diffraction peaks may be observed in the sample with 7% SnO_2. The growing crystallisation of cassiterite is shown in the SEM micrographs of Figure 7.c.

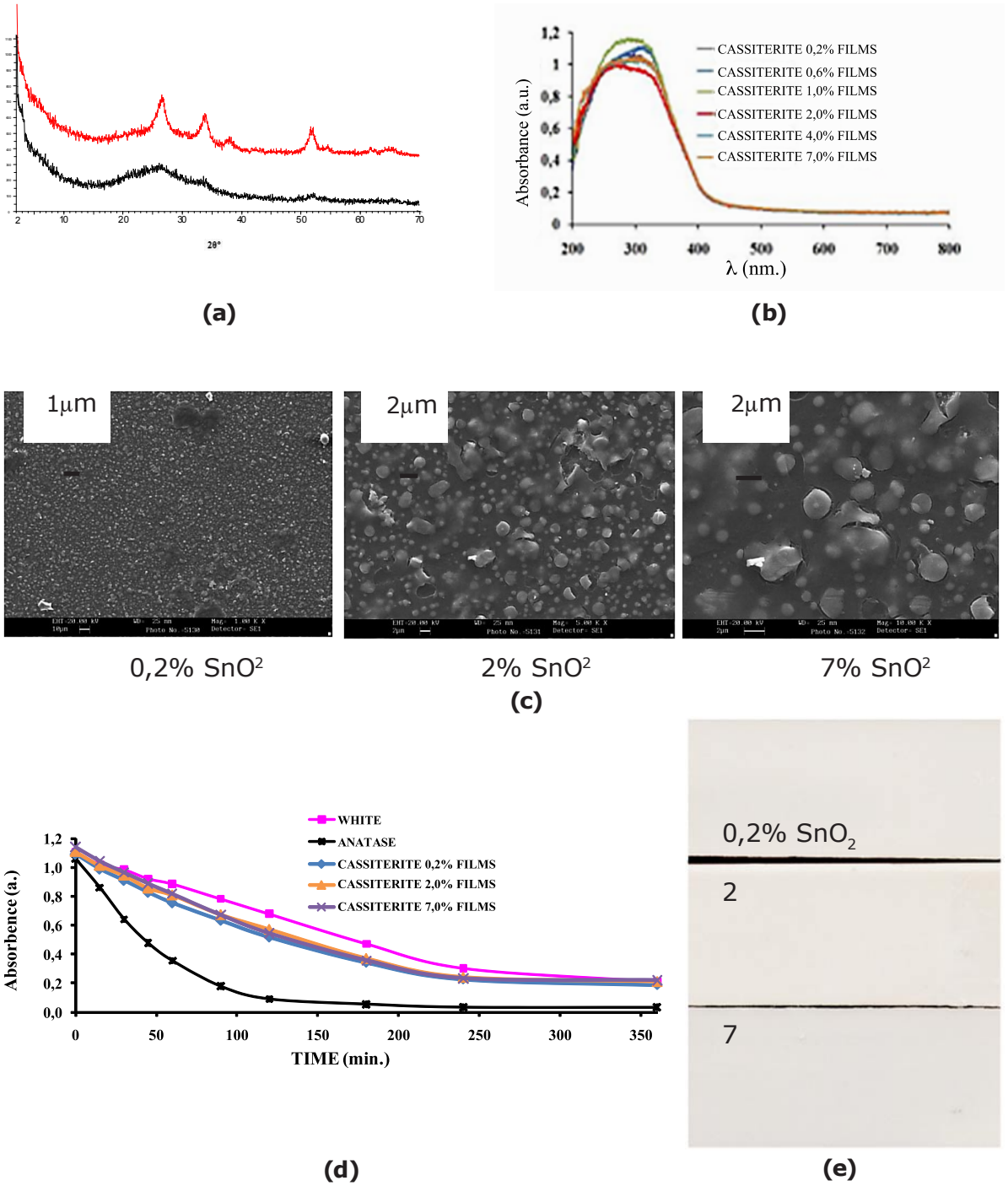

Figure 7. (a) X-ray diffraction of the glaze films; (b) UV-Vis-NIR Spectrum; (c) SEM micrographs; (d) Orange II photodegradation test, (e) photograph of the pieces with the deposited film.

Figure 7.b shows the UV-Vis-NIR spectrum of the different prepared samples. The presence of absorption bands centred at about 290 and 285 nm may be observed. The semiconductor band gap, which was similar in all cases, was about 3.5 eV (Table III).

The photodegradation curves of the Orange II solutions of the films (Figure 7.d) exhibited no significant variation with tin content and the half-life times were

about 110 minutes as may be observed in Table III for all samples, highlighting a moderate activation of the photolytic process. However, when the deposition of anatase from inks with titanium alkoxides was used, the half-life time was only 34 min (9).

SnO_2 (%)	Eg (eV)	R^2	$t_{1/2}$ (min.)
7	3.59	0.890	112
0.2	3.59	0.900	110

Table III. Band gap and Langmuir-Hinshelwood kinetics results for films with 0.2 and 7% SnO_2.

5.2. Tile with photocatalytic glaze

Finally, photocatalysts can also be used in the form of a conventional photocatalytic glaze coating deposited as a glaze composition on a ceramic tile (10). Table IV presents the approximate mass composition of a glaze that devitrifies cassiterite SnO_2, with an average oxide content of 5%. Glazes were prepared with an increasing SnO_2 content, from 3% to 13% added to a crystalline base glaze.

Components	% by weight
SiO_2	58
Al_2O_3	8
K_2O	4.5
CaO	11.5
ZnO	13
SnO_2	5

Table IV. Composition of the glaze that devitrifies cassiterite, SnO_2 (5%).

% SnO_2	Eg (eV)	R^2	$t_{1/2}$ (min.)
13	3.50	0.991	85
11	3.48	0.993	84
9	3.45	0.990	82
7	3.43	0.997	81
5	3.41	0.993	79
3	3.40	0.990 0.983*	78 16*
Crystalline	3.71	0.994	130
Anatase	3.0	0.991 0.992	42 12*
White	------	0.993	151

(*) with relation to methylene blue.

Table V. Calculated parameters of the glaze that devitrifies cassiterite compared with those of the crystalline base glaze and other references.

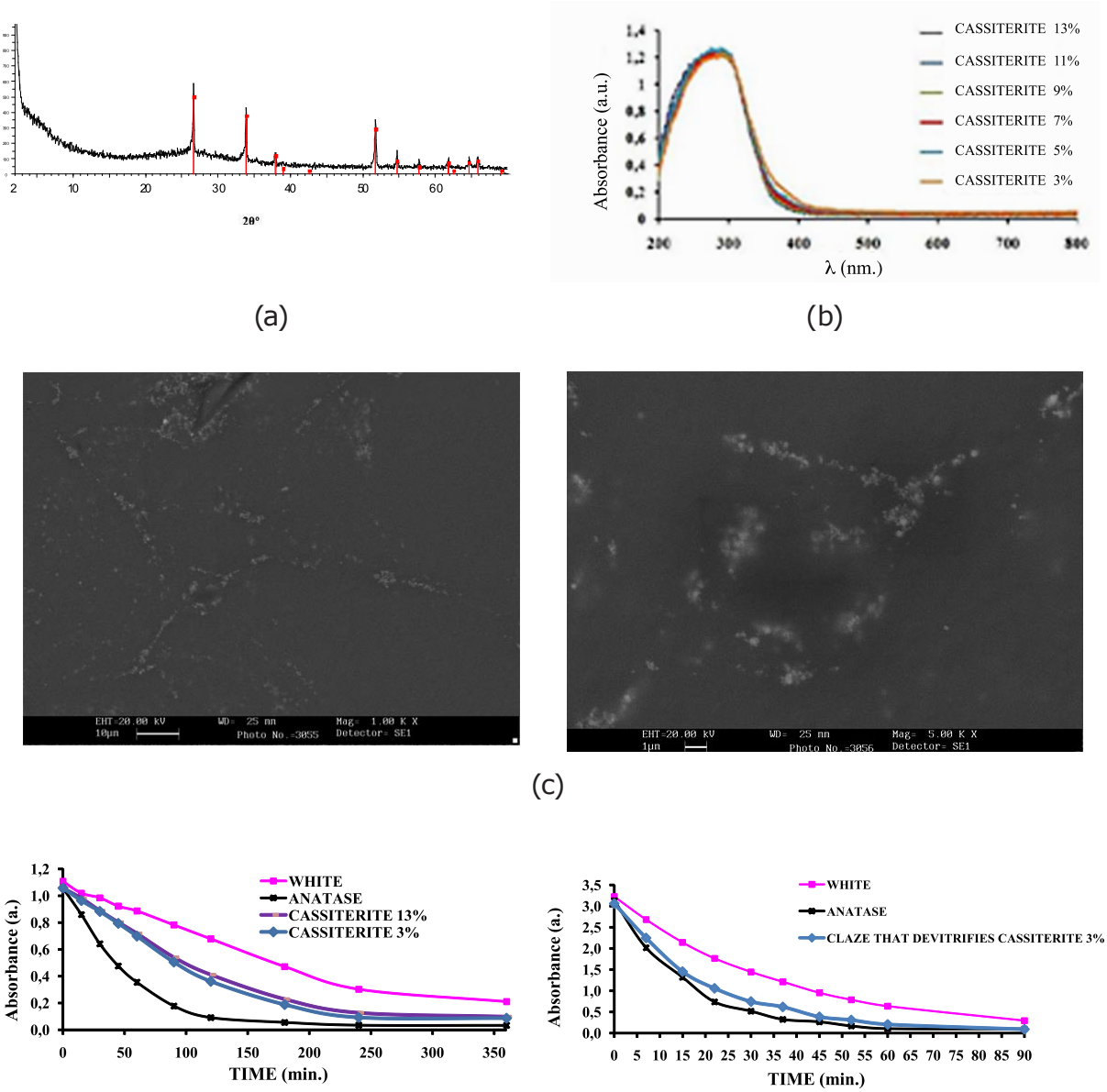

Figure 8. Glaze that devitrifies cassiterite, SnO_2: (a) X-ray diffraction of the fired coating with peaks associated with cassiterite (sample SnO_2 3% by weight); (b) UV-Vis-NIR spectra of the series; (c) SEM micrographs (sample SnO_2 13% by weight); (d) Orange II photodegradation test (samples SnO_2 3% and 13% by weight); (e) Methylene blue photodegradation test (sample SnO_2 3% by weight).

Figure 8.a shows the grazing-angle X-ray diffractions of the fired coating (sample SnO_2 3% by weight); peaks associated with cassiterite, SnO_2, of intermediate intensity are observed. Figure 8.b presents the UV-Vis spectra of the fired coatings that devitrified cassiterite, SnO_2 (samples SnO_2 3% and 13% by weight). Figure 8.c presents SEM micrographs of the glaze at different magnifications of the sample with 13% SnO_2; a thin devitrification in the form of grains is observed with a radius of 100 nm, which gives rise to aggregates of 1 μm diameter. Figure 8.d depicts the Orange II photodegradation curves for this glaze (samples SnO_2 3% and 13% by weight), while Figure 8.e shows the same test but on methylene blue (sample SnO_2 3% by weight).

Table V presents a summary of the calculated parameters obtained of the band gap energy of the UV-Vis spectra of the materials and the values of the degradation kinetics obtained by means of the Langmuir-Hinshelwood model. The values in Table V indicate a half-life time for the photodegradation test obtained by the Langmuir-Hinshelwood model of 78 minutes for Orange II and 16 minutes for methylene blue, for the sample with 3% SnO_2, which are comparable to those of the reference powder anatase (42 and 12 minutes, respectively). When the concentration of cassiterite increased, the band gap grew slightly and so did the half-life time of the Orange II photodegradation. The devitrified cassiterite on the crystalline glaze with particle sizes of order of the 100 nm was photocatalytically more efficient than that obtained by deposition of a cassiterite film described in section 5.1 with larger particle sizes, of the order of the 300 nm in the case of 0.2% SnO_2 (Fig. 7.c).

6. CONCLUSIONS

The results described above highlight the great capability evidenced by the use of 'ceramic' photocatalysts (ceramic composites) in the treatment processes of specific urban environmental pollutants (VOCs and NOx) and of wastewaters (PBT organic compounds), as well as the use 'in ceramics' of glazed ceramic tiles as substrates for photocatalytic layers or photocatalytic glaze coatings.

ACKNOWLEDGEMENTS

The authors gratefully thank the Fundación Bancaja-UJI (Project P1-1B2010-09) and the Ministry of Education (Project MEC 05I403) for the funding received to conduct the study.

REFERENCES

[1] I.S.A. Isaksen, S.B. Dalsøren, Getting a better estimate of an atmospheric radical, Science 331 (2011) 31-39.

[2] C.Gargori, R.Galindo, M. Llusar, M.A. Tena, G. Monrós, J. A. Badenes, Photocatalytic degradation of Orange II by titania addition to sol-gel glasses, J. of Sol-Gel Sci. and Tech., 50(2009)314-320.

[3] Ichiura, H., Kitaoka, T., Tanaka, H.. "Photocatalytic oxidation of NOx using composite sheets containing TiO_2 and a metal compound". Chemosphere 51 (2003)855.

[4] R. Galindo, Vidriados cerámicos Fotoactivos, Tesis Doctoral, Universitat Jaume I, Noviembre 2008.

[5] Wang et al., Environ. Int. 33(2007)694-705.

[6] (a) Directiva 2008/50/CE, de 21 de mayo, relativa a la calidad del aire ambiente y a una atmósfera más limpia en la Unión Europea, (b) Real Decreto 102/2011, de 28 de enero, relativo a la mejora de la calidad del aire.

[7] J.S. Dalton, P.A. Janes, N.G. Jones, J.A. Nicholson, K.R. Hallam, G.C. Allen, Photocatalytic oxidation of NOx gases using TiO_2: a surface spectroscopic approach, Environmental Pollution 120 (2002) 415–422.

[8] I.K. Konstantyinou, T.A. Albanis, TiO_2-assisted photocatalytic degradation of azo dyes in aqueous solution: kinetic and mechanistic investigations. A review, App. Catalyst B: Environmental 49(2004)1-14.

[9] O. Ruiz, F. Sanmiguel, C. Gargori, F. Galindo, G. Monrós, Estudio de la capacidad de degradación fotocatalítica de vidriados cerámicos, QUALICER 2008, ISBN 978-84-95931-31-, PBC15-33, 2008.

[10] S. Meseguer, F. Galindo, S. Sorlí, C.Gargori, M.A.Tena, G.Monrós, Vidriados cerámicos con actividad fotoquímica: aplicación potencial a depuración ambiental, Cerámica Información, 333 (2006)61-68mica: aplicación potencial a depuración ambiental, Cerámica Información, 333 (2006)61-68